



Published in final edited form as:

*Anal Chem.* 2010 January 15; 82(2): 516–522. doi:10.1021/ac901706f.

## Improved HILIC LC/MS of Heparinoids using a Chip with Post-column Make-up Flow

Gregory O. Staples<sup>1</sup>, Hicham Naimy<sup>1</sup>, Hongfeng Yin<sup>2</sup>, Kevin Kileen<sup>2</sup>, Karsten Kraiczek<sup>3</sup>, Catherine E. Costello<sup>1</sup>, and Joseph Zaia<sup>1,\*</sup>

<sup>1</sup>Boston University School of Medicine, Dept. of Biochemistry, Mass Spectrometry Resource, 670 Albany St., Boston, MA 02118

<sup>2</sup>Agilent Laboratories, Agilent Technologies, 5301 Stevens Creek Blvd., MS 3L-WA, Santa Clara, CA 95051

<sup>3</sup>Agilent Technologies, Hewlett-Packard-Str. 8, 76337 Waldbronn, Germany

### Abstract

Heparan Sulfate (HS) and heparin are linear, heterogeneous carbohydrates of the glycosaminoglycan (GAG) family that are modified by *N*-acetylation, *N*-sulfation, *O*-sulfation, and uronic acid epimerization. HS interacts with growth factors in the extracellular matrix, thereby modulating signaling pathways that govern cell growth, development, differentiation, proliferation, and adhesion. HPLC-chip-based hydrophilic interaction liquid chromatography/mass spectrometry has emerged as a method for analyzing the domain structure of GAGs. However, analysis of highly sulfated GAG structures deca-saccharide or larger in size has been limited by spray instability in the negative-ion mode. This report demonstrates that addition of post-column make-up flow to the amide-HPLC-chip configuration permits robust and reproducible analysis of extended GAG domains (up to degree of polymerization 18) from HS and heparin. This platform provides quantitative information regarding oligosaccharide profile, degree of sulfation, and non-reducing chain termini. It is expected that this technology will enable quantitative, comparative glycomics profiling of extended GAG oligosaccharide domains of functional interest.

### Introduction

Heparan Sulfate (HS) and heparin are linear polysaccharides of the glycosaminoglycan (GAG) family. They are biosynthesized as co-polymers with a repeating unit of 4GlcA $\beta$ 1,4-GlcNAc $\alpha$ 1, which is first extended and then modified by a series of reactions in the Golgi.<sup>1, 2</sup> After chain extension, some acetate groups of GlcNAc are replaced with sulfate by *N*-deacetylase *N*-sulfotransferase (NDST) enzymes. This reaction creates substrates for 5'-uronosyl epimerase, responsible for epimerization of GlcA to IdoA, as well as a variety of sulfotransferases that can add sulfate to the 2*O*-position of IdoA and the 6*O*- position of glucosamine. Rare 3*O*-sulfation of glucosamine as well as 2*O*-sulfation of GlcA also occurs.

Heparin is produced by and stored in mast cells, and in its final form is expressed as a free glycan following enzymatic cleavage from the serglycin core protein. For heparin, the *N*-sulfation, epimerization, and *O*-sulfation modifications go nearly to completion. Thus, IdoA2*S*-GlcNS6*S* is the most abundant disaccharide unit. In contrast to heparin, HS is expressed on the surface of nearly all mammalian cells and is conjugated to HS

\*Address correspondence to: Prof. Joseph Zaia Mass Spectrometry Resource Dept. of Biochemistry, Boston University school of Medicine 670 Albany St. Rm. 509 Boston, MA 02118 Tel: 617-638-6762 Fax: 617-638-6761 jzaia@bu.edu.

proteoglycan (HSPG) core proteins. HS displays a lower degree of *N*-sulfation than does heparin, which is likely a function of the specificity and expression level of NDST isoforms in the tissue from which the HS originates.<sup>1</sup> The biosynthetic reactions that polymerize and modify HS chains create domains within the nascent chain characterized by specific *N*-substituents.<sup>3</sup> NA domains are defined by contiguous *N*-acetylated disaccharides and NS domains are defined by contiguous *N*-sulfated disaccharides. NA/NS domains consist of a mixture of *N*-acetylated and *N*-sulfated disaccharides. HS from different organs displays unique domain structures,<sup>4</sup> and the organ-specific structures of HS are conserved from one individual to another.<sup>5, 6</sup> As well, the domain structures of HS are expressed in a spatially and temporally regulated manner.<sup>7</sup> Taken together, these properties make HS an extremely information-rich biomolecule.<sup>8</sup>

As a result of its ability to bind and modulate the activity of a multitude of protein partners, HS plays a role in many biological processes.<sup>9, 10</sup> Physiological concentrations of growth factors are low, and, in some cases, *e.g.* the binding of fibroblast growth factor (FGF) to its receptor, HS is a requisite factor.<sup>11</sup> Its ability to bind both protein partners enables HS to serve as a catalyst of physical interactions<sup>12</sup> between growth factors and their receptors. For FGF signaling in *Drosophila* tracheal development, receptor binding is dependent on either 2*O*- or 6*O*- sulfation patterns.<sup>13</sup> Other binding events depend on more specific modifications. For example, a certain class of neurons requires C5-epimerization patterns for proper axonal patterning in *C. elegans*.<sup>14</sup> Even more specific binding interactions have been documented in the cases of antithrombin III and the gD glycoprotein of *Herpes simplex* virus.<sup>1, 15</sup> It is becoming clear that there is a range in structural requirements for binding between HS and its protein partners.

The structures of NS domains have been implicated as significant determinants in the binding of HS to protein partners.<sup>16</sup> NS domains are typically 3–8 disaccharides in length<sup>17</sup> and contain the highest degree of *O*-sulfation and C5-epimerization modifications, a property resultant from the fact that these reactions are enhanced by *N*-sulfation of GlcN residues.<sup>7</sup> It is known that NS domains interact with protein components such as FGFs.<sup>18</sup> NS domains are thought to be flanked by NA/NS domains, which contain both *N*-sulfated and *N*-acetylated disaccharides.<sup>19</sup> These domains of high or intermediate sulfation alternate with lowly sulfated NA domains. This model of HS domain structure is summarized in Figure 1, which shows a hypothetical HSPG.

Structural analysis of the various domains of HS is necessary for determining their biological activities, but these experiments have been limited by the extreme heterogeneity of this GAG class. Many analytical methods focus on disaccharide analysis of depolymerized GAGs using capillary electrophoresis<sup>20, 21</sup> or chromatography.<sup>22, 23</sup> Mass spectrometry (MS) is now emerging as the method of choice for GAGdisaccharide analysis.<sup>24–26</sup> The importance of the information provided by these experiments cannot be understated, but analysis of larger structures is essential for full understanding of the role of HSPGs in cell regulation.

Capillary amide hydrophilic interaction chromatography (HILIC) with on-line electrospray ionization (ESI) MS has been used for analysis of released glycans,<sup>27</sup> glycopeptides,<sup>28</sup> glycosphingolipids,<sup>29</sup> and GAGs.<sup>30–32</sup> This method has also been utilized for analysis of ATIII binding heparin hexamers,<sup>33</sup> and most recently has been adapted to an HPLC-chip format for analysis of heparin and HS oligosaccharides.<sup>34</sup> The HPLC-chip integrates a 15 cm × 75 μm analytical column, a trapping column, and an electrospray tip.<sup>35, 36</sup> Positioning of the spray needle is robotically controlled, which minimizes the need for optimization of spray conditions, while the integrated trapping column eliminates weakly binding contaminants present in glycan mixtures. Using the HILIC-chip, it was possible to analyze

heparin oligosaccharides up to degree of polymerization (dp) 10 and lowly sulfated HS oligosaccharides up to dp12.<sup>34</sup>

Many glycan and glycoconjugate classes are acidic, owing to the presence of sialic acid or uronic acid residues and/or the presence of sulfate or phosphate groups. Use of negative mode ESI is a natural choice for these glycan classes due to their propensity to form anions in solution. The primary factor that limits the range of compounds that may be analyzed using chip-based negative ESI LC/MS is maintaining spray in solvents having high aqueous content. Such solvent conditions are required for elution of large, polar glycans from an amide HILIC column. This is particularly true for GAGs, because the polarity of a given oligosaccharide increases with increasing length and sulfate content. In our previous work with standard amide-HILIC chips, we noted that highly sulfated HS dp10s begin eluting at a time when the source voltage can no longer maintain electrospray. Though the source voltage can be increased to account for the increasing aqueous content, optimization of this parameter is laborious and requires adjusting during the course of long experiments. Electrospray of very high aqueous content buffer requires spray voltages that exceed safe operating conditions for instrument electronics and the chip apparatus. Thus, there is a physical limitation on the analysis of increasingly polar GAG oligosaccharides when using standard amide-HILIC chips.

This report demonstrates a novel amide-HILIC HPLC-chip that allows introduction of make-up flow (MUF) to the effluent of the analytical column. The MUF chip represents an improvement over standard HPLC-chips because it permits electrospray in high aqueous conditions during negative-ion mode LC/MS. The chip eliminates the need to raise spray voltages as aqueous content increases; a single voltage setting provides stable spray throughout an LC run that reaches conditions of 100% aqueous. We used this chip for analysis of dp10–dp14 HS as well as dp14–18 heparin oligosaccharides, experiments that could not be performed with a standard amide-HILIC HPLC-chip. This robust method of negative-ion LC/MS permits analysis of highly modified GAG domains implicated in numerous biological processes.

## Materials and Methods

Porcine intestinal mucosa heparin was purchased from Sigma-Aldrich (St. Louis, MO). Porcine intestinal mucosa HS was purchased from Celsus Laboratories (Cincinnati, OH). Heparin lyases I and III from *Flavobacterium heparinum* were purchased from Ibex (Montreal, QC). Arixtra (C<sub>31</sub>H<sub>53</sub>N<sub>3</sub>O<sub>49</sub>S<sub>8</sub>) was purchased from Organon Sanofi-Synthelabo LLC (West Orange, NJ). The Arixtra preparation was dialyzed using a 100 Da MWCO before LC/MS analysis.

### Heparanoid Oligosaccharides

Partial digestion of porcine intestinal mucosa heparin (100 mg) was performed in 1 mL of 100 mM ammonium acetate containing 0.1 mg/mL BSA at 37°C. Heparin lyase I was added in 150 milliunit aliquots at 6-h intervals until the digestion reached 30% completion. Digestion progress was monitored by UV absorbance at 232 nm. Complete digestion of porcine intestinal mucosa HS (100 mg) was performed in 1 mL of 100 mM sodium acetate, 5 mM calcium acetate, pH 7.0 at 37°C. Heparin lyase III was added in 30 milliunit aliquots at 6-h intervals until the digestion reached 100% completion. Digestion progress was monitored by UV absorbance at 232 nm. The heparin and HS digests were applied to a 170 cm × 1.5 cm preparative size exclusion chromatography column packed with Bio-Gel P-10 (Bio-Rad, Hercules, CA). The mobile phase had an ionic content of 200 mM ammonium bicarbonate and the column flow rate was 40 µL/min. Size fractions containing heparin or HS were combined and desalted by dialysis using a 100 Da MWCO.

## MUF-chip-based amide-HILIC LC/MS

Amide-80 stationary phase (Tosoh Bioscience, Montgomeryville, PA, 5  $\mu\text{m}$  particle size, 80  $\text{\AA}$  pore size) was packed into an HPLC-chip with a 75  $\mu\text{m}$   $\times$  150 mm analytical column by Agilent Technologies (Santa Clara, CA). The chip contained a 500-nL trapping column and an additional channel allowing introduction of post-column MUF. The HPLC-chip source was coupled to an Agilent 1200 series HPLC system with three pumps. A microscale pump controlled sample loading through the trapping column while a nanoscale pump controlled the gradient through the analytical column. An additional nanoscale pump provided the post-column MUF.

The HPLC mobile phases were as follows: solvent A was 10% acetonitrile, 50 mM formic acid, pH 4.4 and solvent B was 95% acetonitrile, 5% solvent A. Samples (40 pmol total of heparin oligosaccharide mixture or 100 pmol total of HS oligosaccharide mixture) were loaded onto the trapping column with a solvent composition of 74% B at 4  $\mu\text{L}/\text{min}$  for a period of 10 min. Afterwards, the trapping column was placed in-line with the analytical column and a gradient from 74% B to 0% B was run over a period of 39 min at 200 nL/min. Following the gradient, the trapping column and analytical column were washed with 0% B for 10 min. The return to initial conditions was made over 10 min, followed by 10 min of equilibration. A 200 nL/min MUF of acetonitrile was supplied during the entire run. The HPLC-chip system was on-line with an Agilent 6520 QTOF operating in the negative-ion mode. The ion source voltage was set to 1450 V for the entirety of the LC/MS run.

Data files were analyzed using the “find compounds by formula” function of MassHunter software. The files were queried for all possible compounds, as defined by their elemental compositions, within a given dp. Resultant extracted ion chromatograms (EICs) were user-integrated. Summed mass spectra produced from each chromatogram were inspected manually to ensure accurate oligosaccharide identification.

## Results

Maintenance of spray stability is a key challenge in LC/MS analysis of compound classes, such as GAGs, that require the negative-ion mode. The use of a chip-based platform for amide-HILIC LC/MS greatly reduced spray stability problems as compared to standard electrospray devices.<sup>34</sup> The polarity of a given GAG oligosaccharide increases in direct proportion to its size and degree of sulfation, requiring higher aqueous percentages for elution. In standard chip-based amide-HILIC LC/MS, higher spray voltages are required as the percentage of aqueous buffer increases. This entails optimization of spray voltages for gradients that approach high aqueous conditions, but high spray voltage magnitudes in the negative mode need to be avoided to minimize the risk of damage to the chip's electrospray tip or instrument electronics.

To achieve spray stability in both high and low percentage aqueous solvents in the negative-ion mode, a modified HPLC chip was fabricated, as shown in Figure 2. The chip contains an additional flow path supplied by a previously unused port on the HPLC-chip source. The new flow path allows introduction of post-column MUF. The MUF joins the effluent of the analytical column in a junction just before the electrospray tip. Acetonitrile was chosen as the MUF solvent and its effect on system performance was evaluated by repeated injections of the octasulfated pentasaccharide Arixtra under different flow conditions, as shown in Figure 3. As a control, the MUF chip was run at the standard analytical flow rate of 400 nL/min with no MUF added. Addition of 400 nL/min of MUF resulted in significantly decreased ion signal. To address this problem, the flow rate of the analytical column was lowered to 100 nL/min with 300 nL/min of MUF. This substantially increased sensitivity over control conditions, but caused peak tailing, necessitating excessive run times to achieve

adequate chromatographic resolution. Fully optimized LC conditions were found to require a balance of analytical column flow rate, column performance, and absolute intensity of signal from the test molecule. An analytical flow rate of 200 nL/min with a MUF rate of 200 nL/min was selected. Under these conditions, stable spray could be maintained during an LC gradient that reached 100% aqueous conditions. Additionally, the gradient could be performed at a single spray voltage, completely eliminating the need for optimization of this source setting. Stable spray is permitted under these conditions because the solvent mixture exiting the electrospray tip has a lower aqueous content than does the mixture exiting the analytical column.

Bacterial lyases from *Flavobacterium heparinum* are useful enzyme reagents for generating depolymerized products from HS and heparin.<sup>37</sup> As a means of investigating extended, highly sulfated domains, oligosaccharides from porcine intestinal mucosa heparin were generated with heparin lyase I. This enzyme is specific for GlcNS( $\pm$ 6S)-IdoA2S disaccharide repeats, and a partial digest was employed to create oligosaccharides of varying length. The preparation was size-fractionated and oligosaccharides corresponding to dp14, dp16, and dp18 were desalted and analyzed. These oligosaccharides were among the largest that we could fractionate by preparative size exclusion chromatography.

Figure 4a shows the distribution of detected heparin dp14, dp16, and dp18 oligosaccharides from three separate LC/MS experiments. The abundances of the structures are shown as a function of the neutral mass of the detected compound. The distributions are asymmetric and display a negative skew due to the higher abundance of highly sulfated oligosaccharides compared to lowly sulfated oligosaccharides within a given dp. The majority of disaccharides in heparin are *N*-sulfated, and the enhanced activity of *O*-sulfotransferases on *N*-sulfated regions likely explains the distribution observed for these heparin oligosaccharides.<sup>7</sup>

In order to investigate HS domain structures, HS from porcine intestinal mucosa was fully depolymerized with heparin lyase III. This enzyme can cleave between disaccharides of the type GlcNS/NAc( $\pm$ 6S)-GlcA/IdoA, but has strong preference for GlcNAc( $\pm$ 6S)-GlcA. Complete digestion of HS with heparin lyase III thus results in depolymerization of NA and NA/NS domains, and leaves NS domains intact.<sup>19</sup> The depolymerization products were subjected to size-fractionation before analysis by LC/MS. The abundances of oligosaccharides corresponding to dp10, dp12, and dp14 are shown in Figure 4b. These oligosaccharides represent the largest NS domains that we could purify by preparative size exclusion chromatography from this particular HS source. A striking feature of these data is the difference in distribution pattern as compared to the heparin oligosaccharides. The pattern produced by the HS oligosaccharides approximates a Gaussian distribution. This reflects the fact that modifications to HS chains are not as extensive as they are in heparin.

A summed mass spectrum from the LC/MS of HS dp10s is shown in Figure 4c to illustrate the quality of the data produced by this platform. The spectrum is annotated with structures defined by a glycan shorthand, [ $\Delta$ HexA, HexA, GlcN, SO<sub>3</sub>, Ac], that indicates monosaccharide, sulfate, and acetate content. The resolution and mass accuracy of the QTOF used for this work enable precise determination of the heparinoid structures based on accurate mass (typically between  $-3$  and  $+2$  ppm mass error), as shown in supplemental Table S-1. Figure S-1 shows EICs corresponding to selected compounds from Figure 4c. There is a characteristic increase in retention time of each compound as the number of sulfate groups increases.

Figure 5 shows a more detailed presentation of the heparin oligosaccharide data that is summarized in Figure 4a. Only structures containing 0 or 1 Ac were detected in the dp14,



dp16, and dp18 fractions. This is consistent with the high degree of *N*-sulfation reactions that occur during heparin biosynthesis. The data indicated an average degree of sulfation of 2.4 sulfates per disaccharide, and this result matches exactly the previously published data for this type of sample.<sup>38</sup>

The dp10 oligosaccharides produced by lyase III digestion of HS yielded delta-unsaturated ( $\Delta$ -unsaturated) structures containing 1 or 2 Ac groups, as shown in Figure S-2a. These structures originate from the internal region of the HS chain, and the  $\Delta$ -unsaturation is generated by the eliminative mechanism of the heparin lyase. For compounds containing 1 Ac, the most abundant structures have 7 or 8 sulfates, while the most abundant structures for compounds containing 2 Ac have 6 or 7 sulfates. Saturated dp10 oligosaccharides were also detected (Figure S-2b). These structures are produced by the action of a single lyase cleavage and originate from the non-reducing terminus of the HS chain. Interestingly, the distribution of sulfate groups within the detected saturated oligosaccharides was increased by 1 sulfate group compared to the corresponding unsaturated oligosaccharides, indicating a higher degree of sulfation at the non-reducing end of the HS chain.

Analysis of dp12 oligosaccharides produced from lyase III digestion of HS also revealed structures with 1 or 2 Ac, as seen in Figure 6a. For both dp10 and dp12, there were no compounds detected with more than 2 Ac, which is consistent with lyase III generation of NS domains. Compounds with 9 or 10 sulfates were the most abundant structures for  $\Delta$ -unsaturated dp12s containing 1 Ac, while compounds with 8 or 9 sulfates were the most abundant for 2 Ac containing structures. A similar one-sulfate shift in distribution was observed for saturated dp12 structures, as seen in Figure 6b. This, along with the fact that 2 Ac containing saturated structures were lower in abundance when compared to those containing 1 Ac for both dp10 and dp12, indicates that the non-reducing end of the HS chain is more highly sulfated than the internal region. These data parallel previous reports of a highly sulfated non-reducing end of bovine kidney HS.<sup>39</sup> Literature values for average degree of sulfation for HS do not exceed 1 sulfate per disaccharide<sup>40</sup> and typically fall into the range of 0.2–0.7.<sup>41</sup> An average degree of sulfation of 1.48 sulfates per disaccharide was calculated from the HS data on dp10–dp14  $\Delta$ -unsaturated structures. This value reflects the higher sulfate content of NS domains produced under the digestion conditions used for this experiment. Additionally, the data were used to calculate a degree of sulfation of 1.63 sulfates per disaccharide for saturated dp10 and dp12 structures, which quantifies the sulfate content of the non-reducing end.

## Discussion

Heparin is highly sulfated, and may be considered an extended NS domain when compared to HS, which contains long regions of unmodified disaccharides. NS domains from HS can be generated by digestion with heparin lyase III. These heparin-like regions are essential for the protein binding properties of HS. The ability to analyze the structures contained within these domains is essential to understanding the functions of HS in complex biological processes.

Negative-mode ESI is useful for mass spectrometric analysis of GAGs and other acidic glycan classes. A limiting factor in such experiments is the stability of the spray interface in the negative-ion mode, and difficulties in this area have largely been overcome by the use of amide-HILIC HPLC-chips.<sup>34</sup> MUF represents a clear further improvement because the chip-based post-column addition of organic solvent permits electrospray in the negative-ion mode operation during high aqueous chromatographic conditions. Previous attempts to attain stable spray during such gradients, using standard amide-HILIC chips, required raising the spray voltage as the percentage of aqueous solvent increased. This resulted in degradation of

the spray emitter and increased danger of damage to the mass spectrometer electronics through arcing. Oftentimes, spray ignition would be lost during highly aqueous gradients. The addition of MUF to the amide-HILIC chip eliminates the need for time-consuming user optimization. The MUF feature enables stable ESI using a single source voltage even when the gradient reaches 100% aqueous conditions.

We have utilized the MUF amide-HILIC HPLC-chip to characterize NS domains from HS ranging in size from dp10–dp14, as well as heparin oligosaccharides ranging in size from dp14–dp18. For HS, the data indicate a normal distribution of sulfates for a given content of Ac containing oligosaccharides. Of the dp10–dp14 structures analyzed, only 1 Ac or 2 Ac containing compounds were detected, owing to the heparin-like nature of NS domains of HS. Analysis of saturated structures shows evidence of a more highly sulfated non-reducing end, implicating this region in protein binding events. The dp14–dp18 heparin oligosaccharides that were analyzed contain zero or 1 Ac group. For a given Ac content, the oligosaccharides display a sulfation pattern that differs from that observed for HS. The asymmetric distributions show higher abundances for more completely sulfated structures, which is consistent with the highly modified nature of heparin in comparison to HS. These results demonstrate the ability of the system to quantify extended, highly sulfated domains.

MUF amide-HILIC HPLC-chips allow a wide range of HILIC gradients to be performed without ramping of spray voltages to compensate for increasing aqueous content. MUF amide chromatography will be extremely useful for comparative glycomics of long, highly sulfated GAG oligosaccharides. It is anticipated that similar benefits will be observed for analysis of other glycan and glycoconjugate classes using the MUF chips. Additionally, MUF chips should provide advantages when employed in conjunction with other chromatography phases, for example porous graphitized carbon, in the negative-ion mode.

## Supplementary Material

Refer to Web version on PubMed Central for supplementary material.

## Acknowledgments

The authors thank Jose-Angel Mora-Fillat of Agilent Technologies (Waldbronn, Germany) for providing the drawing of the MUF HPLC-Chip. This research is supported by the NIH through Grant No. P41RR10888 and by the Agilent Technologies Foundation through a Research Project Gift.

## Abbreviations

<b>Ac</b>	acetate
<b>dp</b>	degree of polymerization
<b>EIC</b>	extracted ion chromatogram
<b>ESI</b>	electrospray ionization
<b>FGF</b>	fibroblast growth factor
<b>GAG</b>	glycosaminoglycan
<b>GlcA</b>	glucuronic acid
<b>GlcNAc</b>	<i>N</i> -acetylglucosamine
<b>GlcNS</b>	<i>N</i> -sulfoglucosamine
<b>HexA</b>	hexuronic acid

<b>HILIC</b>	hydrophilic interaction chromatography
<b>HPLC</b>	high-performance liquid chromatography
<b>HS</b>	heparan sulfate
<b>HSPG</b>	heparan sulfate proteoglycan
<b>IdoA</b>	iduronic acid
<b>LC/MS</b>	liquid chromatography/mass spectrometry
<b>MUF</b>	make-up flow
<b>MS</b>	mass spectrometry
<b>MWCO</b>	molecular weight cut-off
<b>NDST</b>	<i>N</i> -deacetylase <i>N</i> -sulfotransferase
<b>ppm</b>	parts per million
<b>QTOF</b>	quadrupole time-of-flight mass spectrometer

## References

- (1). Esko JD, Selleck SB. *Annu Rev Biochem.* 2002; 71:435–471. [PubMed: 12045103]
- (2). Bulow HE, Hobert O. *Annu Rev Cell Dev Biol.* 2006
- (3). Esko JD, Lindahl U. *J Clin Invest.* 2001; 108:169–173. [PubMed: 11457867]
- (4). Maccarana M, Sakura Y, Tawada A, Yoshida K, Lindahl U. *J Biol Chem.* 1996; 271:17804–17810. [PubMed: 8663266]
- (5). Ledin J, Staatz W, Li JP, Gotte M, Selleck S, Kjellen L, Spillmann D. *J Biol Chem.* 2004; 279:42732–42741. [PubMed: 15292174]
- (6). Lindahl B, Eriksson L, Lindahl U. *Biochem J.* 1995; 306(Pt 1):177–184. [PubMed: 7864807]
- (7). Lindahl U, Kusche-Gullberg M, Kjellen L. *J Biol Chem.* 1998; 273:24979–24982. [PubMed: 9737951]
- (8). Nugent MA. *Proc Natl Acad Sci U S A.* 2000; 97:10301–10303. [PubMed: 10984527]
- (9). Capila I, Linhardt RJ. *Angew Chem Int Ed Engl.* 2002; 41:391–412. [PubMed: 12491369]
- (10). Conrad, HE. *Heparin-binding proteins.* Academic Press; San Diego: 1998.
- (11). Pellegrini L. *Curr Opin Struct Biol.* 2001; 11:629–634. [PubMed: 11785766]
- (12). Lander AD. *Matrix Biol.* 1998; 17:465–472. [PubMed: 9881597]
- (13). Kamimura K, Koyama T, Habuchi H, Ueda R, Masu M, Kimata K, Nakato H. *J Cell Biol.* 2006; 174:773–778. [PubMed: 16966419]
- (14). Bulow HE, Hobert O. *Neuron.* 2004; 41:723–736. [PubMed: 15003172]
- (15). Shukla D, Liu J, Blaiklock P, Shworak NW, Bai X, Esko JD, Cohen GH, Eisenberg RJ, Rosenberg RD, Spear PG. *Cell.* 1999; 99:13–22. [PubMed: 10520990]
- (16). Carlsson P, Presto J, Spillmann D, Lindahl U, Kjellen L. *J Biol Chem.* 2008; 283:20008–20014. [PubMed: 18487608]
- (17). Turnbull J, Powell A, Guimond S. *Trends Cell Biol.* 2001; 11:75–82. [PubMed: 11166215]
- (18). Kreuger J, Prydz K, Pettersson RF, Lindahl U, Salmivirta M. *Glycobiology.* 1999; 9:723–729. [PubMed: 10362842]
- (19). Murphy KJ, Merry CL, Lyon M, Thompson JE, Roberts IS, Gallagher JT. *J Biol Chem.* 2004; 279:27239–27245. [PubMed: 15047699]
- (20). Hitchcock AM, Bowman MJ, Staples GO, Zaia J. *Electrophoresis.* 2008; 29:4538–4548. [PubMed: 19035406]
- (21). Militopoulou M, Lamari FN, Hjerpe A, Karamanos NK. *Electrophoresis.* 2002; 23:1104–1109. [PubMed: 11981858]



- (22). Toyoda H, Kinoshita-Toyoda A, Fox B, Selleck SB. *J Biol Chem*. 2000; 275:21856–21861. [PubMed: 10806213]
- (23). Toyoda H, Kinoshita-Toyoda A, Selleck SB. *J Biol Chem*. 2000; 275:2269–2275. [PubMed: 10644674]
- (24). Saad OM, Ebel H, Uchimura K, Rosen SD, Bertozzi CR, Leary JA. *Glycobiology*. 2005; 15:818–826. [PubMed: 15843596]
- (25). Shi X, Zaia J. *J Biol Chem*. 2009; 284:11806–11814. [PubMed: 19244235]
- (26). Desaire H, Sirich TL, Leary JA. *Anal Chem*. 2001; 73:3513–3520. [PubMed: 11510812]
- (27). Wuhrer M, Koeleman CA, Deelder AM, Hokke CH. *Anal Chem*. 2004; 76:833–838. [PubMed: 14750882]
- (28). Wuhrer M, Koeleman CA, Hokke CH, Deelder AM. *Anal Chem*. 2005; 77:886–894. [PubMed: 15679358]
- (29). Zarei M, Kirsch S, Muthing J, Bindila L, Peter-Katalinic J. *Anal Bioanal Chem*. 2008; 391:289–297. [PubMed: 18327675]
- (30). Akiyama H, Shidawara S, Mada A, Toyoda H, Toida T, Imanari T. *J Chromatogr*. 1992; 579:203–207. [PubMed: 1429967]
- (31). Hitchcock AM, Yates KE, Costello CE, Zaia J. *Proteomics*. 2008; 8:1384–1397. [PubMed: 18318007]
- (32). Hitchcock AM, Yates KE, Shortkroff S, Costello CE, Zaia J. *Glycobiology*. 2007; 17:25–35. [PubMed: 16980326]
- (33). Naimy H, Leymarie N, Bowman MJ, Zaia J. *Biochemistry*. 2008; 47:3155–3161. [PubMed: 18260648]
- (34). Staples GO, Bowman MJ, Costello CE, Hitchcock AM, Lau JM, Leymarie N, Miller C, Naimy H, Shi X, Zaia J. *Proteomics*. 2009
- (35). Yin H, Killeen K. *J Sep Sci*. 2007; 30:1427–1434. [PubMed: 17623422]
- (36). Yin H, Killeen K, Brennen R, Sobek D, Werlich M, van de Goor T. *Anal Chem*. 2005; 77:527–533. [PubMed: 15649049]
- (37). Ernst S, Langer R, Cooney CL, Sasisekharan R. *Crit Rev Biochem Mol Biol*. 1995; 30:387–444. [PubMed: 8575190]
- (38). Hook M, Lindahl U, Iverius PH. *Biochem J*. 1974; 137:33–43. [PubMed: 4206909]
- (39). Wu ZL, Lech M. *J Biol Chem*. 2005; 280:33749–33755. [PubMed: 16079142]
- (40). LeBrun LA, Linhardt RJ. *Methods Mol Biol*. 2001; 171:353–361. [PubMed: 11450249]
- (41). Rabenstein DL. *Nat Prod Rep*. 2002; 19:312–331. [PubMed: 12137280]

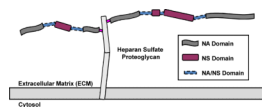


**Figure 1.** Current model of HS domain structure. The reactions responsible for HS biosynthesis create regions of *N*-sulfation (NS domains), *N*-acetylation (NA domains), and regions of mixed *N*-sulfation and *N*-acetylation (NA/NS domains). NS domains are likely flanked by NA/NS domains.

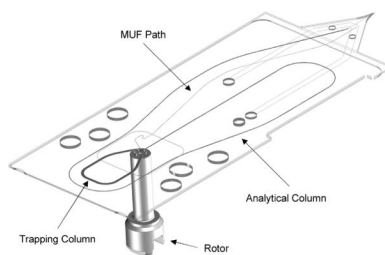


**Figure 2.** MUF HPLC-Chip design. The MUF HPLC-chip is a variation on standard HPLC-chips.<sup>35</sup> An additional laser ablated channel runs from a previously unused inlet port and joins its flow to the analytical column effluent before the electro-sprayer. The chips utilized for this work have a 500-nL trapping column.

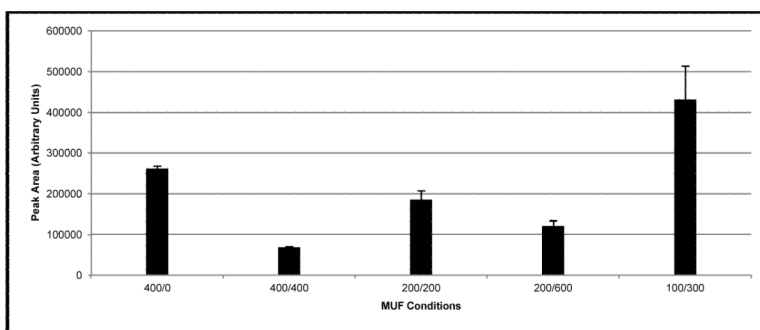


**Figure 3.** Optimization of MUF Amide-HILIC LC/MS. The effect of MUF on sensitivity is shown for various combinations of flow rates. Data is based signal intensity produced by Arixtra (triplicate injections, 2 pmol each). Conditions are designated by ### / ### = analytical column flow rate / MUF rate in nL/min.



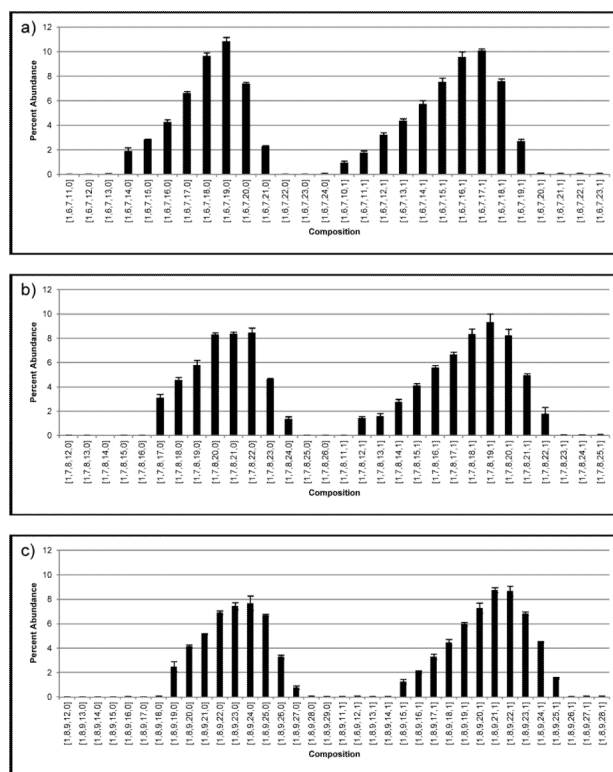


**Figure 5.** MUF amide-HILIC LC/MS of heparin dp14–18 (triplicate injections, 100 pmol each) from 30% heparin lyase I digestion. (a) Relative abundances of  $\Delta$ -unsaturated dp14s (b) Relative abundances of  $\Delta$ -unsaturated dp16s (c) Relative abundances of  $\Delta$ -unsaturated dp18s. Oligosaccharide compositions are given as [ $\Delta$ HexA, HexA, GlcN, SO<sub>3</sub>, Ac].



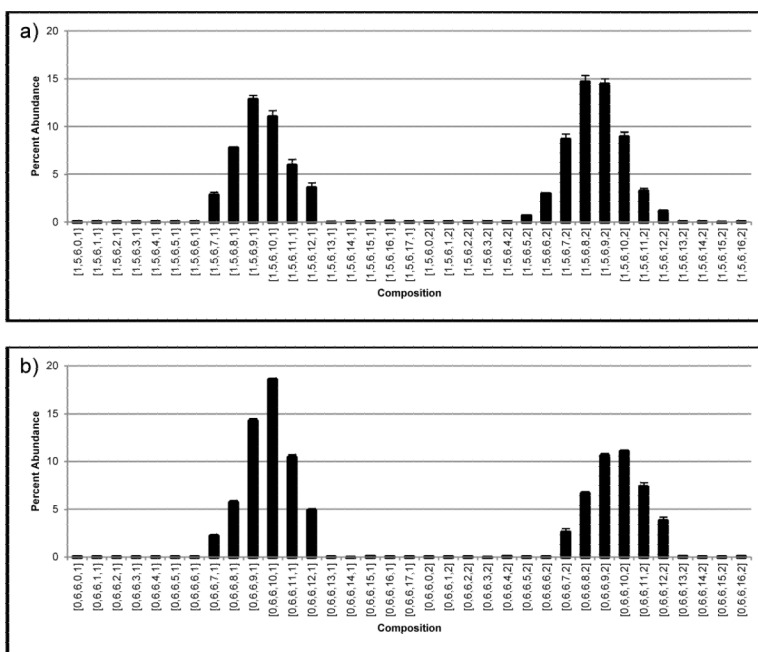


**Figure 6.** MUF amide-HILIC LC/MS of HS dp12s (triplicate injections, 40 pmol each) from heparin lyase III digestion. (a) Relative abundances of  $\Delta$ -unsaturated dp12s (b) Relative abundances of saturated dp12s. Oligosaccharide compositions are given as [ $\Delta$ HexA, HexA, GlcN, SO<sub>3</sub>, Ac].